Nature of Intra-night Optical Variability of BL Lacertae

Haritma Gaur[1]*, Alok C. Gupta[2,1], R. Bachev[3], A. Strigachev[3], E. Semkov[3], M. Böttcher[4,5],
Paul J. Wiita[6], J. A. de Diego[7], Minfeng Gu[1], H. Guo[1], R. Joshi[8], B. Mihov[3], N. Palma[5],
S. Peneva[3], A. Rajasingam[5], L. Slavcheva-Mihova[3]

[1] *Key Laboratory for Research in Galaxies and Cosmology, Shanghai Astronomical Observatory, Chinese Academy of Sciences,*
80 Nandan Road, Shanghai 200030, China; haritma@shao.ac.cn
[2] *Aryabhatta Research Institute of Observational Sciences (ARIES), Manora Peak, Nainital – 263002, India*
[3] *Institute of Astronomy and National Astronomical Observatory,Bulgarian Academy of Sciences,*
72 Tsarigradsko Shosse Blvd., 1784 Sofia, Bulgaria
[4] *Centre for Space Research, North-West University, Potchefstroom 2520, South Africa*
[5] *Astrophysical Institute, Department of Physics and Astronomy, Ohio University, Athens, OH 45701, USA*
[6] *Department of Physics, The College of New Jersey, P.O. Box 7718, Ewing, NJ 08628-0718, USA*
[7] *Instituto de Astronomía, Universidad Nacional Autónoma de México, 04310, México D.F., México*
[8] *Inter-University Centre of Astronomy and Astrophysics (IUCAA), Pune - 411007, India*

ABSTRACT

We present the results of extensive multi-band intra-night optical monitoring of BL Lacertae during 2010–2012. BL Lacertae was very active in this period and showed intense variability in almost all wavelengths. We extensively observed it for a total for 38 nights; on 26 of them observations were done quasi-simultaneously in B, V, R and I bands (totaling 113 light curves), with an average sampling interval of around 8 minutes. BL Lacertae showed significant variations on hour-like timescales in a total of 19 nights in different optical bands. We did not find any evidence for periodicities or characteristic variability time-scales in the light curves. The intranight variability amplitude is generally greater at higher frequencies and decreases as the source flux increases. We found spectral variations in BL Lacertae in the sense that the optical spectrum becomes flatter as the flux increases but in several flaring states deviates from the linear trend suggesting different jet components contributing to the emission at different times.

Key words: galaxies: active – BL Lacertaeertae objects: individual: BL Lacertae – galaxies: photometry

1 INTRODUCTION

BL Lacertae is a well known source which has been used to define a class of active galactic nuclei (AGNs) that, together with flat spectrum radio quasars, make up the highly variable objects called blazars. The BL Lacertae class is characterized by the absence or extreme weakness of emission lines (with equivalent width in the rest frame of the host galaxy of < 5 Å), intense flux and spectral variability across the complete electromagnetic spectrum on a wide variety of time-scales, and highly variable optical and radio polarization (e.g., Wagner & Witzel 1995). A relativistic plasma jet pointing close to our line of sight can account for the

observed properties of these objects. BL Lacertae is an optically bright blazar located at $z = 0.0688 \pm 0.0002$ (Miller & Hawley 1977) hosted by a giant elliptical galaxy with R= 15.5 (Scarpa et al. 2000). BL Lacertae is an LBL (low frequency peaked blazar) as its low energy spectral component peaks at millimeter to micron wavelengths while the high energy spectral component peaks in the MeV-GeV range. On some occasions, BL Lacertae has shown broad $H\alpha$ and $H\beta$ emission lines in its spectrum, raising the issue of its membership in its eponymous class (Vermeulen et al. 1995).

BL Lacertae was observed by several multi-wavelength campaigns carried out by the Whole Earth Blazar Telescope (WEBT/GASP; Böttcher et al. 2003; Villata et al. 2009; Raiteri et al. 2009, 2010, 2013 and references therein). BL

* E-mail: haritma@shao.ac.cn

Lacertae is well known for its intense optical variability on short and intra-day time-scales (e.g. Massaro et al. 1998; Tosti et al. 1999; Clements & Carini 2001; Hagen-Thorn et al. 2004) and strong polarization variability (Marscher et al. 2008; Gaur et al. 2014 and references therein). Extensive light curves for BL Lacertae have been presented by many authors and hence a number of investigations have been carried out to search for the flux variations, spectral changes and any possible periodicities in the light curves (e.g. Racine 1970; Speziali & Natali 1998; Böttcher et al. 2003; Fan et al. 2001; Hu et al. 2006). Nesci et al. (1998) found the source to be variable with the amplitudes of flux variations larger at shorter wavelengths. Papadakis et al. (2003) studied the rise and decay time-scales of the source during the course of a single night and found them to increase with decreasing frequency. They also studied the time-lags between the light curves in different optical bands and found the B band to lead the I band by ∼0.4 hours. Villata et al. (2002) carried out a campaign in 2000–2001 with exceptionally dense temporal sampling, which was able to measure intra-night flux variations of this blazar. They found the optical spectrum to be only weakly sensitive to the long term brightness trend and argued that this achromatic modulation of the flux base level on long time-scales is due to variations of the jet Doppler factor. However, the short-term flux variations and especially the bluer-when-brighter trend indicate the importance of intrinsic processes related to the jet emission mechanism (Raiteri et al. 2013; Agarwal & Gupta 2015).

A key motivation of this study is to look for intra-day flux and spectral variations in optical bands during the active state of BL Lacertae in 2010–2012. We also studied interband BVRI time delays on intra-day time-scales of BL Lacertae. As BL Lacertae is a very well known LBL and the optical bands are located above the first peak of the spectral energy distribution, the fast intra-day variability (IDV) properties can yield rather direct implications for the nature of the acceleration and cooling mechanisms of the relativistic electron populations. Over the course of 3 years, we performed quasi-simultaneous optical multi-band photometric monitoring of this source from various telescopes in Bulgaria, Greece, India and the USA on intra-day time-scales.

The paper is organized as follows. In Section 2 we briefly describe the observations and data reductions. Section 3 discusses the methods of quantifying variability. We present our results in Section 4. Sections 5 & 6 contain a discussion and our conclusions, respectively.

2   OBSERVATIONS AND DATA REDUCTION

Our observations of BL Lacertae started on 10 June 2010 and ran through 26 October 2012. The entire observation log is presented in Table 1. The observations were carried out at seven telescopes in Bulgaria, Greece, India and the USA. The telescopes in Bulgaria, Greece and India are described in detail in Gaur et al. (2012, Table 1) and the standard data reduction methods we used at each telescope are given in Section 3 of that paper, so we will not repeat them here. During our observations, typical seeing vary between 1–3 arcsec. In our observations of BL Lacertae, comparison stars are observed in the same field as the blazar and their

magnitudes are taken from Villata et al. (1998). We used star C for calibration as it has both magnitude and colour close to those of BL Lacertae during our observations.

At the MDM Observatory on the south-west ridge of Kitt Peak, Arizona, USA, data were taken for limited periods during the nights of 3, 4, 5, 6, 7 and 8 July 2010 with the 1.3 m McGraw-Hill Telescope, using the Templeton CCD with B, V, R, and I filters. CCD parameters are described in Table 2. The standard data reduction was performed using IRAF [1], including bias subtraction and flat-field division. Instrumental magnitudes of BL Lacertae plus four comparison stars in the field (Villata et al. 1998) were extracted using the IRAF package DAOPHOT[2] with an aperture radius of 6 arcsec and a sky annulus between 7.5 and 10 arcsec.

The host galaxy of BL Lacertae is relatively bright, so, in order to remove its contribution from the observed magnitudes, we first dereddened the magnitudes using the Galactic extinction coefficient of Schlegel et al. (1998) and converted them into fluxes. We then subtracted the host galaxy contribution from the observed fluxes in R band by considering different aperture radii used by different observatories for the extraction of BL Lacertae magnitudes, using Nilsson et al. (2007). We inferred the host galaxy contribution in B, V and I bands by adopting the elliptical galaxy colours of V−R = 0.61, B−V = 0.96 and R−I = 0.70 from Fukugita et al. (1995). Finally, we subtracted the host galaxy contribution in the B, V and I bands in order to avoid host contamination in the extraction of colour indices.

3   VARIABILITY DETECTION CRITERION

3.1   Power Enhanced F-test

The F-test, as described by de Diego (2010), provides a standard criterion for testing for the presence of intra-night variability. The F-statistic is defined as the ratio of two given sample variances such as s_Q^2 for the blazar instrumental light curve measurements and s_*^2 for that of the standard star, i.e.,

$$F = \frac{s_Q^2}{s_*^2}. \tag{1}$$

Usually, two comparison stars in the blazar field are used to calculate F_1 and F_2, and evidence of variability is claimed if both the F-tests simultaneously reject the null hypothesis at a specific significance level (usually 0.01 or 0.001) (Gaur et al. 2012 and references therein). In this case, the number of degrees of freedom for each sample, ν_Q and ν_* will be the same, and equal to the number of measurements, N minus 1 ($\nu = N - 1$).

Recently, de Diego (2014) called this procedure the "Double Positive Test" (DPT) and pointed out a problem with this procedure that DPT has very low power and in practice its significance level can not be calculated. Also, a large brightness difference or some variability in one of the

---

stars may lead to an underestimation of the source's variability with respect to the dimmer or less variable star. To avoid this issue we employed the power-enhanced F-test using the approach of de Diego (2014) and de Diego et al. (2015). It consists of increasing the number of degrees of freedom in the denominator of the F-distribution by stacking all the light curves of the standard stars and it consists in transforming the comparison star differential light curves to have the same photometric noise as if their magnitudes matched exactly the mean magnitude of the target object. The mean brightness of both the comparison star and the target object are matched to ensure that the photometric errors are equal. Including multiple standard stars reduces the possibility of false detections of intra-night variability that can be produced by one single peculiar comparison star light curve. More details are provided in de Diego et al. 2015. In the analysis, we used three standard stars B, C and H in the field of BL Lacertae whose brightnesses are very close to the brightness of BL Lacertae. Thus, for the ith observation of the light curve of standard star j, for which we have N_j data points, we calculate the square deviation as:

$$s_{j,i}^2 = (m_{j,i} - \overline{m}_j)^2. \qquad (2)$$

By stacking the results of all observations on the total of k comparison stars, we can calculate the combined variance as:

$$s_c^2 = \frac{1}{(\sum_{j=1}^{k} N_j) - k} \sum_{j=1}^{k} \sum_{i=1}^{N_j} s_{j,i}^2. \qquad (3)$$

Then, we compare this combined variance with the blazar light curve variance to obtain the F value with $\nu_Q = N - 1$ degrees of freedom in the numerator and $\nu_* = k(N - 1)$ degrees of freedom in the denominator. This value is then compared with the $F_{\nu_Q, \nu_*}^{(\alpha)}$ critical value, where α is the significance level set for the test. The smaller the α value, the more improbable it is that the result is produced by chance. If F is larger than the critical value, the null hypothesis (no variability) is discarded. We have performed the F-test at the $\alpha = 0.001$ level.

3.2 Discrete Correlation Function (DCF)

To estimate the variability time-scales in the observed light curves of BL Lacertae and to determine the cross-correlations between different optical bands, we used the Discrete Correlation Function (Edelson & Krolik 1988; Hovatta et al. 2007).

The first step is to calculate the unbinned correlation (UDCF) using the given time series by:

$$UDCF_{ij} = \frac{(a(i) - \bar{a})(b(j) - \bar{b})}{\sqrt{\sigma_a^2 \sigma_b^2}}. \qquad (4)$$

Here $a(i)$ and $b(j)$ are the individual points in two time series a and b, respectively, $\bar{a}$ and $\bar{b}$ are respectively the means of the time series, and σ_a^2 and σ_b^2 are their variances. The correlation function is binned after calculation of the UDCF. The DCF can be calculated by averaging the UDCF values (M in number) for each time delay $\Delta t_{ij} = (t_{yj} - t_{xi})$ lying in the range $\tau - \frac{\Delta\tau}{2} \leqslant t_{ij} \leqslant \tau + \frac{\Delta\tau}{2}$ via

$$DCF(\tau) = \frac{1}{n} \sum UDCF_{ij}(\tau). \qquad (5)$$

where τ is the centre of a time bin and n are the number of points in each bin. DCF analysis is frequently used for finding the correlation and possible lags between multifrequency AGN data. When the same data train is used, so $a=b$, there is obviously a peak at zero lag and is called Auto Correlation Function (ACF), indicating that there is no time lag between the two but any other strong peaks in the ACF give indications of variability timescales.

4 RESULTS

4.1 Flux variations

We extensively observed the source for a total of 38 nights during 2010–2012. During 26 of those nights, we observed the source quasi-simultaneously in the B, V, R and I bands, providing a total of 113 light curves in B, V, R and I. These light curves are displayed in Figs. 1 and 2. The lengths of the individual observations were usually between 2 and 6 hours. It is clear from the figures that BL Lacertae was variable from day to day and also on hourly time-scales. We searched for genuine flux variations on IDV time-scales and found 50 light curves to be variable in the whole set of filters during a total of 19 nights using the enhanced F-test. The intranight variability amplitudes (in per cent) are given by Heidt & Wagner (1996):

$$Amp = 100 \times \sqrt{(A_{max} - A_{min})^2 - 2\sigma^2}, \qquad (6)$$

where A_{max} and A_{min} are the maximum and minimum values in the calibrated light curves of the blazar, and σ is the average measurement error. The enhanced F-test values are presented in Table 1.

The duty cycle (in per cent) (DC) of BL Lacertae is computed following the definition of Romero et al. (1999) that later was used by many authors (e.g., Stalin et al. 2004; Goyal et al. 2012, and references therein),

$$DC = 100 \frac{\sum_{i=1}^{n} N_i(1/\Delta t_i)}{\sum_{i=1}^{n} (1/\Delta t_i)}, \qquad (7)$$

where $\Delta t_i = \Delta t_{i,obs}(1 + z)^{-1}$ is the duration of the monitoring session of a source on the ith night, corrected for its cosmological redshift, z. Since for a given source the monitoring durations on different nights are not always equal, the computation of the DC is weighted by the actual monitoring duration Δt_i on the ith night. N_i is set equal to 1 if intra-day variability was detected by the F-test (given in Table 1), otherwise $N_i = 0$. We found the duty cycle of BL Lacertae to be around 44 per cent.

4.2 Amplitude of Variability

When the variability is substantial the amplitude of variability usually is greater in higher energy bands (B) and smaller in lower energy bands (R) in most of the observations. It has been found by many investigators that amplitude of variability is greater at higher frequencies for BL Lacertaes (Ghisellini et al. 1997; Massaro et al. 1998; Bonning et al. 2012) however, the amplitude of variability is not systemaically larger at higher frequencies is also found on some occasions (Ghosh et al. 2000; Ramirez et al. 2004). In few cases, we found the amplitude of variability

in lower energy bands to be comparable to or greater than the amplitude of variability in higher energy bands. Still, because the errors in the B band are higher in these cases, while they are often lower in the lower frequency band, there are some nights during which the statistical significance of the variations falls below our thresholds in B (also sometimes V), when clear variability is detected in R and I bands. Also, differences in the amplitude of variability in various optical bands change from one observation to another. The highest fractional amplitude of variability was found to be ∼38 per cent on 6 July 2010, where the source showed a ∼0.3 mag change in less than 3.5 hours in V band.

We searched for possible correlations between the variability amplitude and the duration of the observation, as displayed in Fig. 3 (left panel). We found a significant positive correlation ($\rho = 0.3306$ with $p = 0.0190$, where ρ and p are the Spearman Correlation coefficient and its p-value, respectively) between them, i.e., the variability amplitude increases with duration of the observation. We conclude that there is an enhanced likelihood of seeing higher amplitudes of variability in longer duration light curves, which is in agreement with Gupta & Joshi (2005) report for a larger sample of blazars.

Next we examined the possible correlation between the amplitude of variability with the source flux (Fig. 3, right panel). It can be seen that amplitude of variability decreases as the source flux increases (ρ=-0.4990 with p=0.0002). This might be explained as, if the source attains a high flux state, the irregularities in the jet flow decreases particularly if fewer non-axisymmetric bubbles were carried outward in the relativistic magnetized jets (Gupta et al. 2008). For instance, the blazar 3C 279 was observed in 2006 during its outburst/high state but did not show any genuine microvariability, while other sources which were in their pre/post outburst state showed significant micro-variability (Gupta et al. 2008). This anti-correlation between variability amplitude and flux could also be explained by a two component model where in more active phases or in an outburst state, the slowly varying jet component rises and dominates on the emission from the more variable regions, i.e., shocks/knots, and therefore reduces the fractional amplitude. However, there is scatter in the plot, some of which could be due to an observational bias, as some observations were longer than others. Due to this, the observed variability amplitude at similar luminosities could be quite different as the amplitude of variability increases with the duration of the observation.

4.3   R-band Autocorrelations

We searched for the presence of a characteristic time-scale of variability in all of the nights by auto-correlating the R-band measurements, for which we had the most data. In most of the nights, the auto-correlation function (ACF) shows a sharp maximum at nearly zero lag, as expected, and it stays positively auto-correlated with itself for time lags of somewhat less than 1 hour followed by dropping to negative values. Hence, we conclude that we did not find any evidence for characteristic variability time-scales from this approach. One example of R-band ACF is shown in the left panel of figure 4.

### 4.4   Inter-band cross-correlations

We computed the DCFs to determine the cross-correlations and time delays between the B and I, V and I, and R and I bands. The time delays are expected between emission in different energy bands, as the flare usually begin at higher frequencies and then propagates to lower frequencies in the inhomogeneous jet model. Injected high energy electrons emit synchrotron radiation first at higher frequencies and then cool, emitting at progressively lower frequencies, resulting in time lag between high and low frequencies. The DCFs between the light curves in all bands show close correlations among the various bands in the nights where genuine variability is present. For the nights in which no genuine variability is present, we normally found much weaker correlations between the bands (<0.4). As the peak of the DCFs are broad, we fit the DCFs with Gaussian functions to determine the possible time delays; however, lags indicated by the DCFs are all consistent with zero. This is not surprising due to the closeness of the various optical bands we measured in frequency space, so if any lags are present they appear to be less than the resolution of our light curves. An example of the DCF is shown in the right panel of fig. 4.
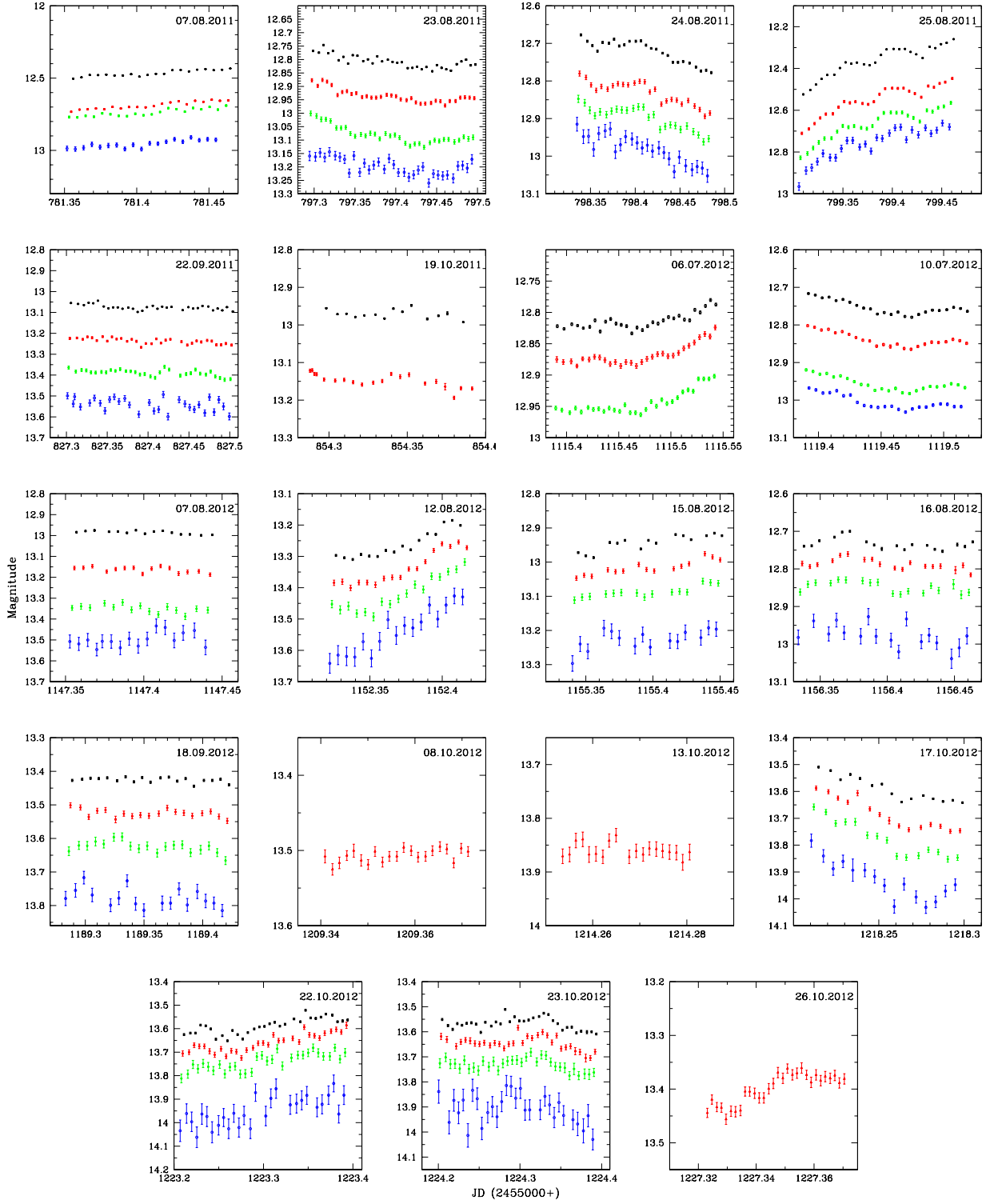
4.5   Colour Indices

We next investigated the existence of spectral variations by studying the behaviour of colour variations with respect to the brightness of BL Lacertae. The colour indices (CIs) are calculated by combining almost simultaneous (within 8 minutes) B, V, R and I magnitudes to yield CIs = B−V, V−R, R−I and B−I. For a particular night, we studied the colour variability only when both light curves were identified as variable. Our data have the advantage of being almost simultaneous in various optical bands. It is important to recall that the underlying host galaxy, effect of the accretion disk component and the Gravitational microlensing can also lead to apparent, but unreal, colour variations (Hawkins 2002). But, since Gravitational microlensing is important on weeks to months time-scales and during our observations, BL Lacertae was in flaring state (Raiteri et al. 2013) where the Doppler boosting flux from the relativistic jet almost invariably swamps out the contribution of the accretion disk component, so we can rule out the contribution of these components. Also, the data we have used in calculating the colour indices are host galaxy subtracted so we conclude that our results indicates variability of the non-thermal continuum radiation.

We studied the variations of colour indices with respect to brightness in 13 of these observations. We fit all the colour–magnitude diagrams with a linear model of the form CI = $m \times$ mag + c (where m is the slope in the fit, V magnitude is taken as mag and c is its respective intercept). The Pearson correlation coefficient (r), its p-value (null hypothesis probability; we consider a confirmed colour index correlation with the V magnitude when p <0.01) along with the slopes and intercepts are presented in Table 3. The significant positive correlations between the colour index and magnitude along with a change of slope >3 σ indicates that the source exhibits a bluer-when-brighter trend.

In five of the nights, which are marked by asterisks in Table 3, we found significant variations in colour indices at
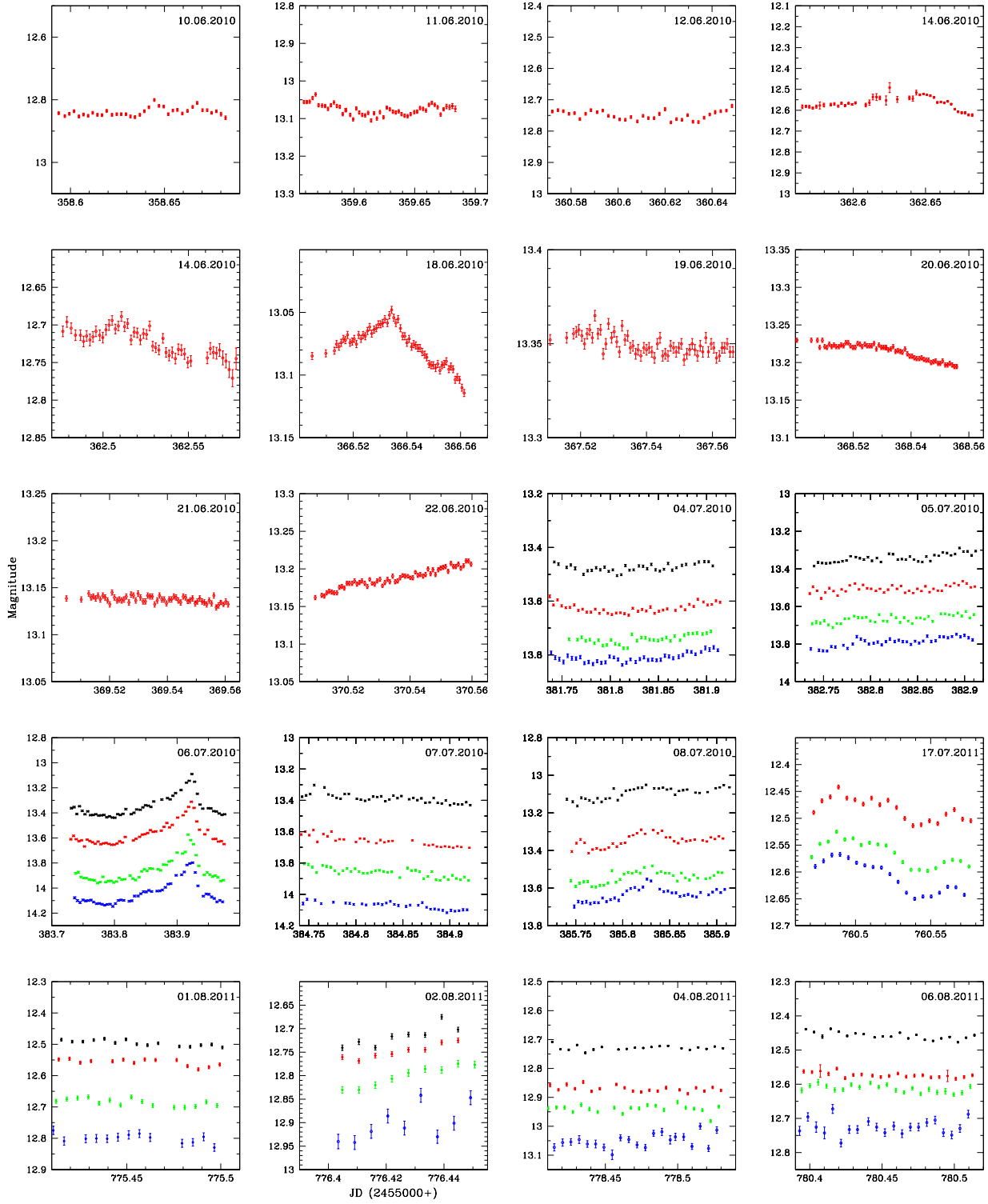
Figure 1. IDV light curves of BL Lacertae during 2010 and early 2011 in the B (blue), V(green), R(red) and I(black) bands. The X-axis is JD (2455000+), and the Y-axis is the calibrated magnitudes in each of the panels. The B, V and I bands are shifted by arbitrary offsets with respect to R-band light curve. Observations from observatory A are represented by squares; those from C are represented by triangles; D by filled circles; E by open circles and F by starred symbols.

Figure 2. As in Fig. 1 for August 2011 through October 2012.

the 3-σ level. In these observations, colour indices correlate with the source brightness and the overall correlation is positive, which indicates hardening of the spectrum as the source brightens. So, in these observations, BL Lacertae exhibits bluer-when-brighter trend with different regression slopes. No significant negative correlations are found for the

source. The bluer-when-brighter tendency in BL Lacertae has been seen by several groups on long-term as well as short-term time-scales (e.g. Papadakis et al. 2003; Villata et al. 2004; Stalin et al. 2006; Larionov et al. 2010; Gu et al. 2006; Gaur et al. 2012; Wierzcholska et al. 2015). Villata et al. (2004) characterized the intra-day flares to be strong
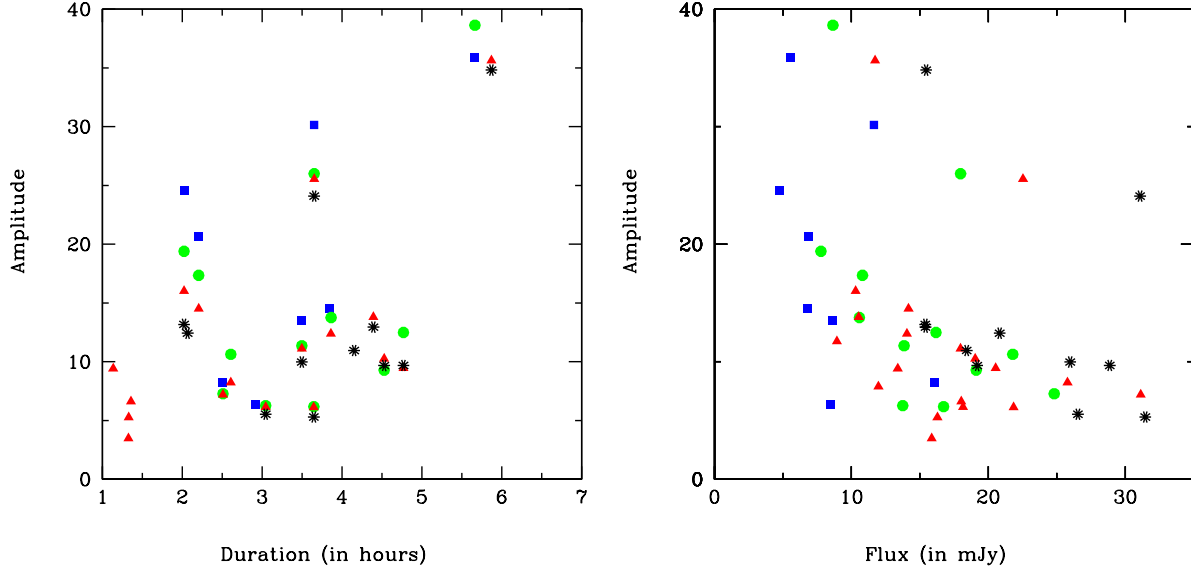
Figure 3. Dependence of amplitude of variability on duration (left panel) and flux (right panel) of the observations. Here, B band is represented by squares (blue), V by solid circles (green), R by triangles (red) and I by starred symbols (black) .
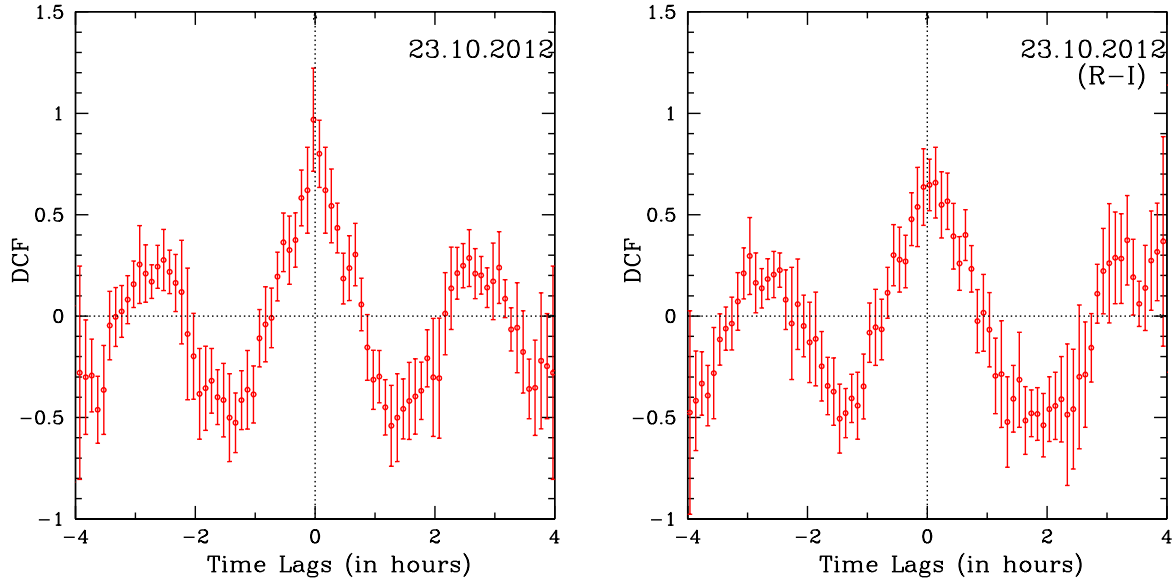
Figure 4. One example of Auto-correlation (R band) is shown in the left figure and DCF (R versus I) is shown in the right figure.

bluer-when-brighter chromatic events with a slope of $\sim$0.4. In five observations, we found a bluer-when-brighter trend with a slope varying between 0.18–0.28 (in Table 3).

In the other eight observations, we did not find significant linear correlations between colour indices and magnitudes (Table 3). In some of them significant colour variations are seen but are not well fitted by linear functions. During the observations on 6 July 2010 (Fig. 1, fourth panel), we found a strong flare with magnitude variation of $\sim$0.3 in all the optical bands and the behaviour of the colour magnitude diagram varies according to the different flux states. But, on intra-day timescales it is difficult to judge the variations of

the colour indices with respect to different brightness states as the flare is on hours like timescales. Also, in other observations, i.e, 8 July 2010, 24 and 25 August 2011, we saw small sub-flares superimposed on the long-term trend. In these cases, the colour indices vary significantly within the individual observations, sometimes showing different branches in the colour magnitude diagrams according to the flux states. Spectral steepening during the flux rise can be explained by the presence of two components, one variable with a flatter slope which dominates during the flaring states and another one that is more stable and contributes to the long term achromatic emission (Villata et al. 2004). So, it could be

Table 2. Details of telescopes and instruments

Telescope:	1.3 m McGraw-Hill Telescope
Chip size:	4064×4064 pixels
Pixel size:	$15 \times 15\ \mu m$
Scale:	$0.315''$/pixel
Field:	$21.3' \times 21.3'$
Gain:	2.2-2.4 e^-/ADU
Read Out Noise:	5 e^- rms

Table 3. Results of linear fits to Colour-Flux Diagrams.

Date of Observation	Band	r	p	c±Δc Intercept	m±Δm Slope
06.07.2010	(B-V)	-0.138	0.339	1.038±0.446	-0.032±0.032
	(V-R)	0.315	0.026	-1.055±0.675	0.110±0.048
	(R-I)	0.023	0.873	0.459±0.675	0.008±0.048
	(B-I)	0.316	0.026	0.442±0.534	0.087±0.038
08.07.2010	(B-V)	-0.106	0.537	1.500±1.455	-0.066±0.105
	(V-R)	0.205	0.230	-1.389±1.540	0.136±0.111
	(R-I)	0.110	0.545	-0.626±1.836	0.085±0.133
	(B-I)	0.220	0.198	-0.516±1.643	0.156±0.119
17.07.2011	(B-V)*	0.629	0.003	-2.424±0.879	0.234±0.068
	(V-R)	0.512	0.021	-1.150±0.627	0.123±0.049
07.08.2011	(V-R)	0.193	0.415	-0.434±1.058	0.067±0.081
23.08.2011	(V-R)*	0.714	<0.001	-3.423±0.670	0.289±0.050
	(R-I)	0.280	0.109	-0.658±0.779	0.096±0.058
24.08.2011	(B-V)	0.057	0.788	0.113±1.910	0.038±0.141
	(V-R)	0.181	0.388	-0.805±1.446	0.094±0.107
	(R-I)	-0.022	0.917	0.787±1.219	-0.009±0.090
	(B-I)	0.264	0.202	0.095±1.269	0.123±0.094
25.08.2011	(B-V)	0.087	0.673	0.235±0.836	0.027±0.063
	(V-R)	0.345	0.118	-0.162±0.366	0.045±0.028
	(R-I)	0.251	0.217	0.051±0.439	0.042±0.033
	(B-I)	0.325	0.105	0.125±0.894	0.114±0.067
06.07.2012	(V-R)*	0.530	0.003	-1.643±0.641	0.159±0.048
	(R-I)*	0.506	0.004	-2.429±0.994	0.231±0.074
10.07.2012	(B-V)	-0.084	0.703	1.019±0.956	-0.027±0.071
	(V-R)	0.061	0.781	0.332±0.550	0.011±0.040
	(R-I)	0.487	0.019	-2.201±1.125	0.212±0.083
	(B-I)	0.395	0.062	-0.850±1.347	0.196±0.099
12.08.2012	(B-V)	0.310	0.243	-2.208±2.320	0.205±0.168
	(V-R)	0.101	0.709	0.052±1.131	0.031±0.082
	(R-I)	0.581	0.011	-1.618±0.861	0.166±0.062
	(B-I)	0.517	0.040	-3.774±2.458	0.402±0.178
17.10.2012	(B-V)	-0.103	0.716	1.370±1.927	-0.051±0.136
	(V-R)*	0.674	0.006	-1.526±0.614	0.142±0.043
	(R-I)*	0.668	0.006	-1.945±0.816	0.186±0.058
	(B-I)	0.542	0.037	-2.102±1.694	0.278±0.120
22.10.2012	(R-I)*	0.482	0.006	-2.203±0.970	0.210±0.071
23.10.2012	(V-R)	0.217	0.233	-1.919±1.973	0.170±0.140
	(R-I)	0.163	0.373	-1.262±2.147	0.137±0.152

*: Significant variations are found in these observations.
r & p: Pearson Correlation Coefficient and its probability values respectively.

possible that during these observations, the superposition of many distinct new variable components lead to the overall weaking of the colour-magnitude correlations. Bonning et al. (2012) studied a sample of FSRQs and BL Lacertaes and found that FSRQs follow redder-when-brighter trends while BL Lacertaes show no such trends. They found complicated behaviour of the blazars on colour-magnitude diagrams: hysteresis tracks, and acromatic flares which depart from the trend suggesting different jet components becoming important at different times. Therefore, our colour variability results show that the intra-night flares between 2010 and early 2012 are chromatic but do not always follow simple bluer-when-brighter trends.

5   DISCUSSION

We performed photometric monitoring of BL Lacertae during the period 2010–2012 for a total of 38 nights in the B, V, R and I bands in order to study its flux and spectral variability. In 19 of those nights, we found genuine IDV. The light curves often show gradual rises and decays, sometimes with smaller sub-flares superimposed. No evidence for periodicity or other characteristic time scales was found. We find the duty cycle of the source during this period to be ∼44%. In the earlier studies, it has been found that LBLs display stronger IDV than HBLs (high frequency peaked blazars) and the DC has been estimated to be ∼70% for LBLs and ∼30–50% for HBLs (Heidt & Wagner 1998; Romero et al. 2002; Gopal-Krishna et al. 2003). Gopal-Krishna et al. (2011) studied a large sample of blazars and found that if variability amplitude (Amp) >3% is considered, the DC is 22% for HBLs and 50% for LBLs. We found DC of ∼44% for BL Lacertae (which is a well known LBL) is in accordance with the previous studies.

In the literature, there are various models which explains intra-day variability of blazars. Intrinsic ones focus on the evolution of the electron energy density distribution of the relativistic paricles leading to a variable synchrotron emission, with shocks accelerating turbulent particles in the plasma jet which then cools by synchrotron emission (e.g., Marscher, Gear & Travis 1992; Marscher 2014; Calafut & Wiita 2015). Extrinsic ones involve geometrical effects like swinging jets where the path of the relativistic moving blobs along the jet deviated slightly from the line of sight, leading to a variable Doppler factor (e.g., Gopal-Krishna & Wiita 1992). The long term periodic and acromatic BL Lacertae variability may be mostly explained by the geometrical scenarios where viewing angle variation can be due to the rotation of an inhomogeneous helical jet which causes variable

Doppler boosting of the corresponding radiation (Villata et al 2002; Larionov et al. 2010 and references therein). As we are considering the faster intra-night flux variations that are associated with the colour variations, they are more likely to be associated with models involving shock propagating in a turbulent plasma jet.

When variability is clearly detected, its amplitude is usually greater at higher frequencies, which is consistent with previous studies (Papadakis et al. 2003; Hu et al. 2006) and can be well explained by electrons that are accelerated at the shock front and then lose energy as they move away from the front. Higher-energy electrons lose energy faster through the production of synchrotron radiation, and are produced in a thin layer behind the shock front. In contrast, the lower-frequency emission is spread out over a larger volume behind the shock front (Marscher & Gear 1985). This leads to time lags of the peak of the light curves toward lower

Table 1. Results of Intra-day Variability of BL Lacertae

Date	Telescope	Band	F_{enh}	$F_c(0.001)$	$Amp\%$	Variable
10.06.2010	A	R	1.018	2.386	-	NV
11.06.2010	A	R	0.985	2.008	-	NV
12.06.2010	A	R	1.034	2.386	-	NV
14.06.2010	A	R	1.054	2.076	-	NV
	C	R	0.934	2.033	-	NV
18.06.2010	E	R	51.328	1.940	6.63	Var
19.06.2010	E	R	1.861	1.940	-	NV
20.06.2010	E	R	21.725	1.930	3.48	Var
21.06.2010	E	R	1.227	1.972	-	NV
22.06.2010	E	R	29.890	1.94	5.28	Var
04.07.2010	F	B	2.164	2.281	-	NV
		V	2.155	2.481	-	NV
		R	0.146	2.236	-	NV
		I	0.938	2.281	-	NV
05.07.2010	F	B	1.527	2.305	-	NV
		V	0.618	2.281	-	NV
		R	0.109	2.258	-	NV
		I	1.052	2.281	-	NV
06.07.2010	F	B	32.4002	1.995	35.85	Var
		V	36.577	1.995	38.64	Var
		R	45.931	2.047	35.64	Var
		I	55.757	1.995	34.82	Var
07.07.2010	F	B	2.307	2.481	-	NV
		V	2.284	2.305	-	NV
		R	1.611	2.258	-	NV
		I	1.247	2.258		NV
08.07.2010	F	B	17.271	2.305	14.49	Var
		V	3.824	2.281	13.76	Var
		R	6.864	2.281	12.40	Var
		I	4.720	2.331	10.96	Var
17.07.2011	E	B	35.089	3.239	8.23	Var
		V	90.629	3.239	7.28	Var
		R	50.931	3.239	7.20	Var
01.08.2011	D	B	1.860	3.932	-	NV
		V	2.774	3.932	-	NV
		R	2.094	3.932	-	NV
		I	1.862	3.932	-	NV
02.08.2011	D	B	1.584	6.195	-	NV
		V	4.858	6.195	-	NV
		R	5.322	7.077	-	NV
		I	2.540	7.077	-	NV
04.08.2011	D	B	0.907	2.849	-	NV
		V	0.552	2.983	-	NV
		R	1.507	2.983	-	NV
		I	1.346	2.983	-	NV
06.08.2011	D	B	0.368	2.736	-	NV
		V	0.300	2.736	-	NV
		R	0.670	2.790	-	NV
		I	0.859	2.849	-	NV
07.08.2011	D	B	0.997	3.239	-	NV
		V	7.058	3.239	10.63	Var
		R	7.773	3.239	8.23	Var
		I	2.046	3.239		NV
23.08.2011	D	B	0.730	2.448	-	NV
		V	4.960	2.448	12.49	Var
		R	8.400	2.448	9.47	Var
		I	5.092	2.448	9.69	Var
24.08.2011	D	B	4.035	2.849	13.55	Var
		V	7.389	2.849	11.36	Var
		R	16.187	2.849	11.12	Var
		I	13.665	2.849	9.98	Var
25.08.2011	D	B	11.247	2.790	30.14	Var
		V	56.7659	2.790	26.30	Var
		R	63.145	2.790	25.55	Var
		I	17.878	2.790	24.10	Var
22.09.2011	D	B	1.354	2.639	-	NV
		V	1.565	2.517	-	NV
		R	1.329	2.517	-	NV
		I	0.930	2.517	-	NV
19.10.2011	D	R	0.574	3.239	-	NV
		I	0.841	4.142	-	NV
06.07.2012	E	V	25.590	2.596	6.18	Var
		R	21.632	2.596	6.14	Var
		I	9.829	2.596	5.30	Var
10.07.2012	E	B	16.174	2.983	6.40	Var
		V	57.750	2.913	6.27	Var
		R	28.700	2.913	6.15	Var
		I	11.878	2.913	5.54	Var
07.08.2012	D	B	2.110	3.753	-	NV
		V	0.558	3.932	-	NV
		R	0.638	3.932	-	NV
		I	0.746	3.932	-	NV
12.08.2012	D	B	4.669	3.598	20.67	Var
		V	18.835	3.598	17.35	Var
		R	36.030	3.598	14.52	Var
		I	24.429	3.753	12.43	Var
15.08.2012	D	B	0.670	3.932	-	NV
		V	0.417	3.932	-	NV
		R	0.908	3.932	-	NV
		I	0.754	3.932	-	NV
16.08.2012	D	B	0.908	3.463	-	NV
		V	1.726	3.463	-	NV
		R	1.622	3.463	-	NV
		I	0.764	3.463	-	NV
18.09.2012	D	B	0.540	3.345	-	NV
		V	1.395	3.345	-	NV
		R	1.034	3.345	-	NV
		I	0.678	3.345	-	NV
08.10.2012	C	R	3.007	1.961	7.89	Var
13.10.2012	C	R	6.686	3.239	11.76	Var
17.10.2012	D	B	6.863	3.932	24.58	Var
		V	27.535	3.932	19.40	Var
		R	42.842	3.932	16.02	Var
		I	33.239	3.932	13.18	Var
22.10.2012	D	B	1.383	2.686	-	NV
		V	1.462	2.555	-	NV
		R	10.608	2.555	13.80	Var
		I	10.043	2.555	12.95	Var
23.10.2012	D	B	0.606	2.596		NV
		V	3.585	2.481	9.29	Var
		R	5.166	2.517	10.25	Var
		I	3.329	2.481	9.68	Var
26.10.2012	C	R	4.330	2.596	9.42	Var

A: 1.04 meter Samprnanand Telescope, ARIES, Nainital, India
D: 60-cm Cassegrain Telescope at Astronomical Observatory Belogradchik, Bulgaria
F: 1.3 m McGraw-Hill Telescope, Arizona, USA
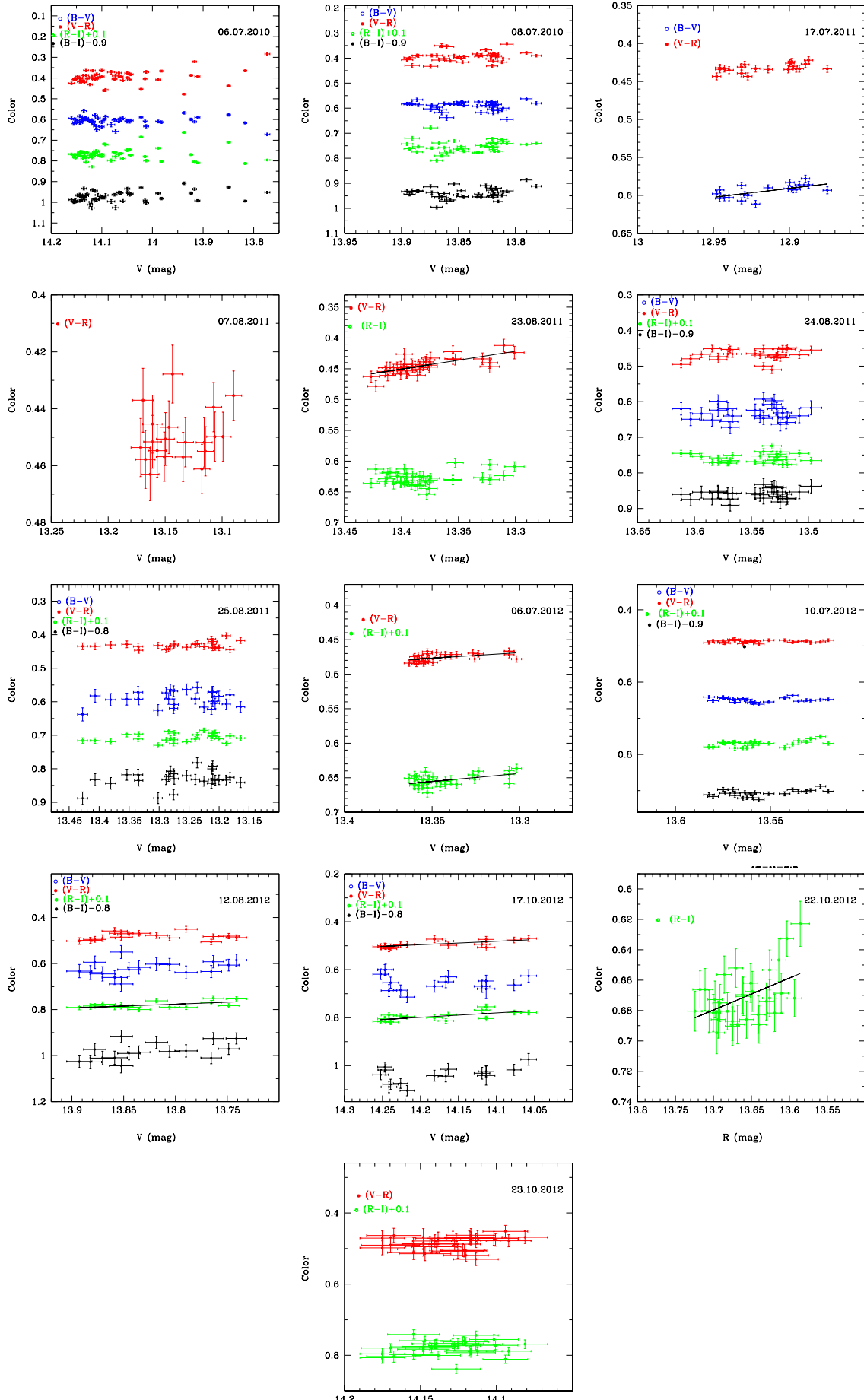F_{enh}: Enhanced F-test values
Amp: Variability Amplitude

C: 50/70-cm Schmidt Telescope at National Astronomical Observatory, Rozhen, Bulgaria
E: 1.3-m Skinakas Observatory, Crete, Greece

$F_c(0.001)$: Critical Values of F Distribution at 0.1%;
Var / NV: Variable / Non-variable

frequencies and amplitude of variability higher at higher frequencies which is clearly visible in the multi-frequency blazars light curves. Due to the closeness of the various optical bands, the starting time of a flare should be almost the same and hence on short time-scales, it is difficult to detect the time lags between the optical bands. Although the amplitude of variability is an inherent property of the source, we had to examine whether it has any dependence on the duration of observation, and found a significant positive correlations between the observed amplitude of variability of the light curves and the duration of the observations. As noted by Gupta & Joshi (2005), on intra-day timescales, the probability of seeing a significant intra-day variability generally increases if the source is continuously observed for long durations. In our observations, duration of monitoring varies between 1.5–5.8 hours. Also, we found that the amplitude of variability decreases as the source flux increases which can be explained as the source flux increases, the irregularities in the turbulent jet (Marscher 2014) decrease and the jet flow becomes more uniform leading to a decrease in amplitude of variability.

We searched for the possible correlations between colour versus magnitude and found significant positive correlations between them in five of the observations out of total 13. So, BL Lacertae showed significant bluer-when-brighter trends on these night with different regression slopes (in Table 3). This behaviour is very well known for BL Lacertaes and can be interpreted as resulting from rapid, impulsive injection/acceleration of relativistic electrons, followed by subsequent radiative cooling (e.g., Böttcher & Chiang 2002). However, other observations do not show significant linear correlations and show complicated behaviour on colour-magnitude diagrams i.e different slopes according to the different flux states or nearly zero slopes between colour-magnitude (Table 3). Of course it is possible that superposition of different spectral slopes from many variable components (standing shocks in different parts of the jet) could lead to the overall weakening of the colour-magnitude correlations (Bonning et al. 2012).

Hence, the behaviour of the colour–magnitude diagrams provides us with indirect information on the amplitude difference and time-lags between these bands as Dai et al. (2011) performed simulations to confirm that both the amplitude differences and time delays between variations at different wavelengths result in a hardening of the spectrum during the flare rise. They showed that if there is a difference in amplitude in two light curves, it leads to the evolution of the object along a diagonal path in the colour-magnitude diagram. If there is a time-lag along with the amplitude change, counter-clockwise loop patterns on the colour index–magnitude diagram arise (Dai et al. 2011). However, any such lags are probably shorter than the sampling time of our observations, so we are not able to detect them through the DCFs we computed.

6 CONCLUSIONS

Our conclusions are summarized as follows:

● During our observations in 2010-2012 BL Lacertae was highly variable in B, V, R and I bands. The variations were well correlated in all four bands and were very smooth, with gradual rises/decays. In one of the observations, on 6 October 2010, we found a pronounced flare-like event, and the highest variability amplitude is found in the V band at 38 per cent.

● In the cases with significant variability, the amplitude of variability is highest in the highest energy band.

● The amplitude of variability correlates positively with the duration of the observation and decreases as the flux of the source increases.

● We searched for time delays between the B, V, R and I bands in our observations, but we did not find any significant lags. This implies that the variations are almost simultaneous in all of the bands and any time lags, if present, are less than our data sampling interval of ∼8 minutes.

● The flux variations are associated with spectral variations on intra-day time-scales. In 5 of the 13 observations, the optical spectrum showed the overall bluer-when-brighter trend which could well represent highly variable jet emission.

● The colour vs. magnitude diagrams show different behaviours which could represent the contribution of different variable components during the flaring states.

● We conclude that the acceleration and cooling timescales are very short for these optical variations and hence dense optical observations with even shorter cadence and higher sensitivity are required to better characterize them.

REFERENCES

Agarwal A., Gupta A. C., 2015, MNRAS, 450, 541
Bonning E., et al., 2012, ApJ, 756, 13
Calafut V., Wiita P. J., 2014, arXiv, arXiv:1407.3687
Böttcher M., Chiang J., 2002, ApJ, 581, 127
Böttcher M., et al., 2003, ApJ, 596, 847
Clements S. D., Carini M. T., 2001, AJ, 121, 90
Dai Y., Wu J., Zhu Z.-H., Zhou X., Ma J., 2011, AJ, 141, 65
de Diego J. A., 2010, AJ, 139, 1269
de Diego J. A., 2014, AJ, 148, 93

de Diego J. A., Polednikova J., Bongiovanni A., Pérez García A. M., De Leo M. A., Verdugo T., Cepa J., 2015, arXiv, arXiv:1505.02113

Edelson R. A., Krolik J. H., 1988, ApJ, 333, 646

Fan J. H., Qian B. C., Tao J., 2001, A&A, 369, 758

Fukugita M., Shimasaku K., Ichikawa T., 1995, PASP, 107, 945

Gaur H., et al., 2012, MNRAS, 420, 3147

Gaur H., Gupta A. C., Wiita P. J., Uemura M., Itoh R., Sasada M., 2014, ApJ, 781, L4

Ghisellini G., et al., 1997, A&A, 327, 61

Ghosh K. K., Ramsey B. D., Sadun A. C., Soundararajaperumal S., 2000, ApJS, 127, 11

Gopal-Krishna, Wiita P. J., 1992, A&A, 259, 109

Gopal-Krishna, Stalin C. S., Sagar R., Wiita P. J., 2003, ApJ, 586, L25

Gopal-Krishna, Goyal A., Joshi S., Karthick C., Sagar R., Wiita P. J., Anupama G. C., Sahu D. K., 2011, MNRAS, 416, 101

Goyal A., Gopal-Krishna, Wiita P. J., Anupama G. C., Sahu D. K., Sagar R., Joshi S., 2012, A&A, 544, A37

Gu M. F., Lee C.-U., Pak S., Yim H. S., Fletcher A. B., 2006, A&A, 450, 39

Gupta A. C., Joshi U. C., 2005, A&A, 440, 855

Gupta A. C., et al., 2008, AJ, 136, 2359

Hagen-Thorn V. A., et al., 2004, yCat, 903, 243

Hawkins M. R. S., 2002, ASPC, 284, 351

Heidt J., Wagner S. J., 1996, A&A, 305, 42

Heidt J., Wagner S. J., 1998, A&A, 329, 853

Hovatta T., Tornikoski M., Lainela M., Lehto H. J., Valtaoja E., Torniainen I., Aller M. F., Aller H. D., 2007, A&A, 469, 899

Hu S. M., Wu J. H., Zhao G., Zhou X., 2006, MNRAS, 373, 209

S., Madejski G. M., Tashiro M., Urry C. M., Kubo H., 2000, ApJ, 528, 243

Larionov V. M., Villata M., Raiteri C. M., 2010, A&A, 510, A93

Marscher A. P., 2014, ApJ, 780, 87

Marscher A. P., et al., 2008, Natur, 452, 966

Marscher A. P., Gear W. K., 1985, ApJ, 298, 114

Marscher A. P., Gear W. K., Travis J. P., 1992, vob..conf, 85

Massaro E., Nesci R., Maesano M., Montagni F., D'Alessio F., 1998, MNRAS, 299, 47

Miller J. S., Hawley S. A., 1977, ApJ, 212, L47

Nesci R., Maesano M., Massaro E., Montagni F., Tosti G., Fiorucci M., 1998, A&A, 332, L1

Nilsson K., Pasanen M., Takalo L. O., Lindfors E., Berdyugin A., Ciprini S., Pforr J., 2007, A&A, 475, 199

Papadakis I. E., Boumis P., Samaritakis V., Papamastorakis J., 2003, A&A, 397, 565

Racine R., 1970, ApJ, 159, L99

Raiteri C. M., et al., 2009, A&A, 507, 769

Raiteri C. M., et al., 2010, A&A, 524, A43

Raiteri C. M., et al., 2013, MNRAS, 436, 1530

Ramírez A., de Diego J. A., Dultzin-Hacyan D., González-Pérez J. N., 2004, A&A, 421, 83

Romero G. E., Cellone S. A., Combi J. A., 1999, A&AS, 135, 477

Romero G. E., Cellone S. A., Combi J. A., Andruchow I., 2002, A&A, 390, 431

Scarpa R., Urry C. M., Padovani P., Calzetti D., O'Dowd M., 2000, ApJ, 544, 258

Schlegel D. J., Finkbeiner D. P., Davis M., 1998, ApJ, 500, 525

Speziali R., Natali G., 1998, A&A, 339, 382

Stalin C. S., Gopal Krishna, Sagar R., Wiita P. J., 2004, JApA, 25, 1

Stalin C. S., Gopal-Krishna, Sagar R., Wiita P. J., Mohan V., Pandey A. K., 2006, MNRAS, 366, 1337

Tosti G., et al., 1999, BlazD, 2, 1

Vermeulen R. C., Ogle P. M., Tran H. D., Browne I. W. A., Cohen M. H., Readhead A. C. S., Taylor G. B., Goodrich R. W., 1995, ApJ, 452, L5

Villata M., et al., 2002, A&A, 390, 407

Villata M., et al., 2004, A&A, 421, 103

Villata M., et al., 2009, A&A, 501, 455

Wagner S. J., Witzel A., 1995, ARA&A, 33, 163

Wierzcholska A., Ostrowski M., Stawarz Ł., Wagner S., Hauser M., 2015, A&A, 573, A69